FAST WAVE HEATING AND CURRENT DRIVE IN ELMING H–MODE PLASMAS IN DIII–D*

R.I. Pinsker, F.W. Baity,† W.P. Cary, J.S. deGrassie, R.H. Goulding,† N.L. Greenough,‡ M. Murakami,† C. C. Petty, and R. Prater

General Atomics, P.O. Box 85608, San Diego, California 92186-9784 USA

1. Introduction

The DIII–D Fast Wave Current Drive (FWCD) program has concentrated on studying the basic physics of direct electron heating and current drive in low density L–mode discharges from its inception in 1991 through 1996. Among the reasons for this are the controllable low densities that can be achieved in L–mode, thus maximizing the power per particle available with a fixed transmitter power, and the high and nearly steady antenna loading that is obtained, maximizing the coupled rf power levels with a given maximum antenna voltage. Among the principal results of the L–mode experiments [1,2] was the observation of nearly full absorption of the coupled FW power, despite calculated first-pass absorption in the range of 8%–15%. However, the heating and current drive efficiencies dropped off sharply when the calculated first-pass absorption was less than about 8% in the condition studied. This was explained by an unspecified edge loss mechanism at the level of 4% per bounce. A survey of possible edge loss mechanisms in these experiments [3] showed that the most plausible candidate for the important edge loss mechanism was dissipation in far field rectified rf sheaths [4].

The more recent DIII–D FWCD work has been aimed at extension of the operating regimes of the experiments, including higher total power by combining FW with NBI [5] and 110 GHz ECH [6]. Generally, these higher power levels result in H–mode confinement, and in a quasi-steady-state condition, Edge Localized Modes (ELMs). Over the past two years, the DIII–D FWCD systems have been modified to improve their capabilities under a wider range of dynamic antenna loading conditions, such as those characteristic of ELMing H–modes. In this paper, the first results of extending the FWCD studies to ELMing H–mode discharges are presented.

2. Technical Improvements to DIII–D FWCD Systems

The DIII–D FWCD system consists of three four-element antenna arrays, of two different designs, and three transmitters, also of two different designs. The original system (referred to as 285, from the toroidal angle in the DIII–D vessel at which the antenna array is located) was operated at frequencies close to 60 MHz in these experiments, and the two newer systems (referred to as 0 and 180) were used at approximately 83 MHz. A considerable simplification of the 285 system's transmission line that was carried out in 1997 is described in detail in Ref. [7]. The resulting system has only one adjustable tuning element (the “decoupler” stub), yet the standing wave ratio seen by the transmitter is less than 1.25 at all times during the discharge despite rapid fluctuations in the antenna loading resistance of more than a factor of four in ELMing H–mode. One further refinement in the operation of 285 that was used in the

*Work supported by U.S. Department of Energy under Contracts DE-AC03-89ER51114, DE-AC05-96OR22464, and DE-AC02-76CH03073.

†*Oak Ridge National Laboratory.*

‡*Princeton Plasma Physics Laboratory.*

1998 experiments was to adjust the operating frequency, within the instantaneous bandwidth of the transmitter, to compensate for changes in the reactive component of the antenna loading caused by different antenna/plasma gaps. Since this system has no adjustable tuning elements to compensate for these changes, the frequency adjustment (in the range of 59.8–60.1 MHz) is necessary to minimize the power diverted to the dummy load.

The modifications to the two newer systems to enhance their H–mode capabilities were to the arc protection circuits, which were reconfigured to be functionally identical to the older system's. The resulting arc protection system distinguishes rapid load transients that appear symmetrically on all four elements of an array from localized changes in impedance that affect only one element at a time. Impedance changes of the symmetric type occur at L–H transitions and ELMs, or are caused by any other nearly axisymmetric fluctuation, while localized arcs in a single antenna in an array cause impedance changes of the latter type. Furthermore, all three systems are equipped with “balanced fault detectors,” which remove the rf drive when the antenna loading is anomalously high. The principle of this detector was based on the observation of a type of fault which appeared symmetric to all four array elements, but corresponded to a very high resistive loading, much higher than observed even at the peak of an ELM. This fault is interpreted as an rf discharge filling the antenna housing. Balanced faults were sometimes triggered by an ELM, particularly when the plasma surface was close to the antennas, and thereby constituted one limitation on the power that could be reliably coupled to ELMing H–mode discharges.

A 50 ms-long time history showing a typical example of operation of these systems in an ELMing H–mode is shown in Fig. 1. The coupling resistance of all three antenna arrays increases by a factor of between 2.5 and 4 at each ELM (indicated by the increase in the photodiode signal which measures D_α radiation at the plasma edge). Despite this substantial change in the antenna impedance, the power reflection coefficient seen at the transmitter output increases only to about 3%. The fixed pretuning arrangement used on the 285 array (no variable tuning elements other than the decoupler stub) causes the fraction of the transmitter power that is diverted to the dummy load (the waste percentage) to *decrease* at each ELM from about 25% to less than 10%. The tuners that remain in the 0 and 180 systems are adjusted so that the fraction of power diverted to their dummy loads is virtually 0 between ELMs, *increasing* to about 25% at the peak of each ELM. Which of these two configurations is more desirable is not obvious at present; comparison of these configurations is among the technical goals of these experiments. In 1998, the 285 system was reliably operated with a peak rf voltage limit of about 25 kV, while the 0 antenna operated successfully at peak voltages over 30 kV. Operation of the 180 system was limited not by peak antenna voltage, but by transmitter power, as a result of the higher ohmic losses in that system's relatively long transmission lines.

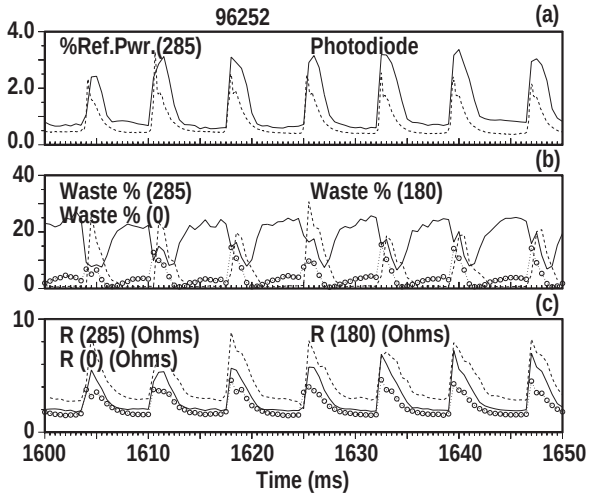

Fig. 1. (a) Time histories of the power reflection coefficient seen by 285 system's transmitter (solid line) and photodiode signal (dashed) in ELMing H–mode discharge. (b) Percentage of power diverted to dummy load for the 285 (solid), 180 (dashed), and 0 (symbols) systems. (c) Coupling resistance for the 285, 180 and 0 (similar labeling) antenna arrays.

3. Electron Heating and Current Drive Experiments in ELMing H–mode Discharges

The first set of systematic experiments on FWCD and electron heating in ELMing H–mode plasmas were performed in the sawtooth-free portion (early neutral beam injection) of 1.4 MA discharges at a toroidal field of 2.05 T in a lower single null divertor configuration. 5 MW of NBI and up to 1.2 MW of 110 GHz ECH [6] were used to produce a target plasma with $T_e(0)$~4.5 keV at a line-averaged electron density of ~3.5×10^{19} m^{-3} with an ELM frequency of ~100 Hz. Discharges were studied with different "outer gaps" (the outer gap is the distance from the separatrix to the limiter at the outboard midplane; the face of the antenna Faraday shields is recessed about 3 cm behind the limiter) between 2.5 and 8 cm, with all other parameters held as constant as possible. The total fast wave power that could be coupled to these discharges was less than 2 MW, owing to the very light antenna loading obtained between ELMs – comparable to only twice the loading obtained in the absence of plasma (half of the net power is coupled to the plasma) at the larger outer gaps. The resistive loading decayed exponentially with the outer gap for all three arrays, as shown in Fig. 2(a). The rate of decay of the loading as the gap was increased was ~60% larger than had been observed in L–mode, which further exacerbated the difficulty of high power coupling at large gaps.

The FW power directly deposited on electrons was measured using standard Fourier techniques by modulating the FW power at 40 Hz (80% modulation depth, square wave envelope) and measuring the correlated response on the electron cyclotron emission (ECE) radiometer channels covering the core of the plasma ($\rho \leq 0.6$). In the case of the 8 cm outer gap, about half of the coupled FW power could be accounted for in this way, which is a fraction comparable to that obtained in previous studies under good absorption conditions. At smaller outer gaps, however, the fraction of the power appearing in the plasma core dropped substantially [Fig. 2(b)]. At an outer gap of 5 cm, the power that could be found in the modulation analysis was somewhat higher in a discharge in which the divertor cryopump was not used compared with a pumped case at the same outer gap. This gap dependence might be expected from a model in which the edge loss due to far field sheaths is the dominant mechanism competing with the weak central absorption due to TTMP and Landau damping: the rf electric field available at the wall to produce the $E_{||}$ that in turn excites the sheaths [4] is exponentially larger at smaller gaps, just as the antenna loading increases at smaller gaps. Furthermore, the electron density at the wall would be expected to be higher at smaller gaps, which also tends to increase the power dissipated in the sheaths.

This trend continued in the FW current drive results. The loop voltage profile as a function of time and the fast wave current drive were deduced by comparing sawtooth-free discharges with co- and counter-current drive antenna phasings, as has been described previously [5]. Up to 80 kA of central FWCD were measured in the 8 cm gap case, as shown in Fig. 3(a); again, the measured driven current declined at smaller gaps, despite the higher coupled FW power. The measured FWCD was compared with code calculations based on the ergodic multipass limit [8], with no assumed edge loss. The results are shown in Fig. 3(b); a substantial edge loss [2] would be required to explain the current drive and heating deficit in the 3.5 cm case. The key point is that the central current drive efficiency, a local quantity, cannot itself depend on the edge plasma conditions. Hence, the measured sensitivity of the

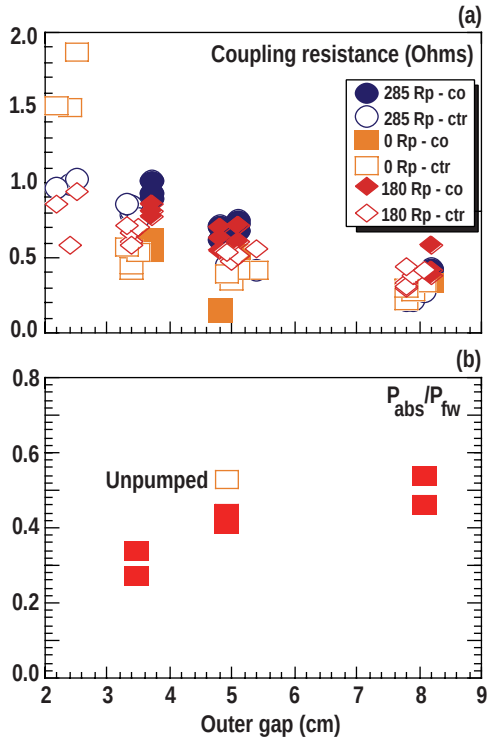

Fig. 2. (a) Coupling resistance for all three antenna arrays (between ELMs) in the outer gap scan. (b) Fraction of coupled fast wave power deposited within $\rho \leq 0.6$ from the ECE modulation analysis.

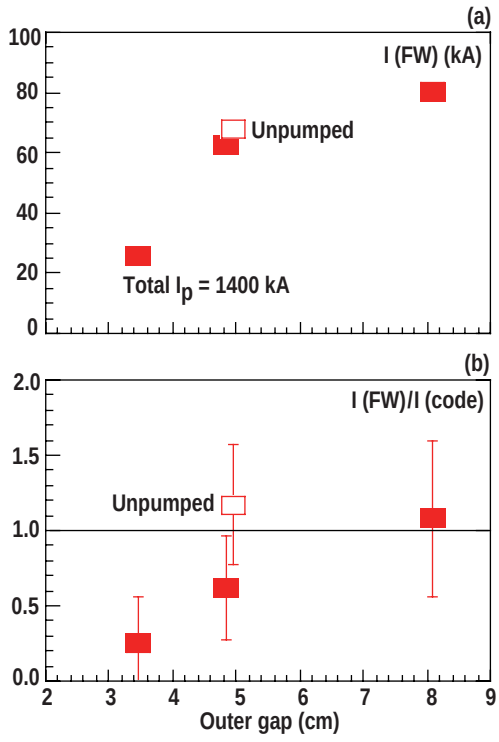

Fig. 3. (a) FW-driven current (co-current phasing) in the outer gap scan. (b) Ratio of measured FW-driven current to that calculated from the multipass code, assuming no edge loss.

driven current to the edge plasma parameters must result from the dependence of the edge loss mechanism that competes with central damping in the multipass limit on edge parameters.

Future experimental work will aim to measure the far-field sheaths directly with probes distant from the fast wave arrays and to investigate the correlation between the sheaths and the edge loss required to account for the measured central electron heating and current drive efficiencies as a function of outer gap. Also, previous observations have shown a relationship between the ELM characteristics and the central heating efficiency. Direct measurement of the sheaths and their dependence on the ELM characteristics should facilitate finding ELMing H–mode conditions that are compatible with efficient high-power central fast wave heating and current drive.

References

[1] R.I. Pinsker, *et al.*, in Proc. 21st EPS Conf., **18B**, Part III, (1994) p. 1118.

[2] C.C. Petty, *et al.*,Nucl. Fusion **35**, 773 (1995).

[3] J.R. Myra and D.A. D'Ippolito, Bull. Am. Phys. Soc. **39**, 1628 (1994).

[4] J.R. Myra, D.A. D'Ippolito and M. Bures, Phys. Plasmas **1**, 2890 (1994).

[5] C.C. Petty, *et al.*, in *Radio Frequency Power in Plasmas* (Proc. 12th Top. Conf., Savannah, 1997), (AIP, New York, 1997) 225.

[6] R. Prater, *et al.*, this conference.

[7] R.I. Pinsker, *et al.*, in Proc. 17th IEEE/NPSS Symp. on Fusion Eng., San Diego, 1997 (IEEE, Piscataway, NJ, to be published); General Atomics Rpt. GA-A22752 (1997).

[8] K. Kupfer, C.B. Forest, C.C. Petty, and R.I. Pinsker, Phys. Plasmas **1**, 3915 (1994).